JOURNAL OF THE MECHANICAL BEHAVIOR OF BIOMEDICAL MATERIALS ▮ (▮▮▮▮) ▮▮▮–▮▮▮

Available online at www.sciencedirect.com

SciVerse ScienceDirect

journal homepage: www.elsevier.com/locate/jmbbm

Research paper

A thermo-mechanical treatment to improve the superelastic performances of biomedical Ti–26Nb and Ti–20Nb–6Zr (at.%) alloys

F. Sun[a,b], Y.L. Hao[c], S. Nowak[b], T. Gloriant[d], P. Laheurte[e], F. Prima[b,*]

[a] Faculty of Materials Science and Chemical Engineering, China University of Geosciences, Wuhan 430074, China
[b] Laboratoire de Physico-Chimie des Surfaces, Groupe de Métallurgie Structurale (UMR 7045), ENSCP, 11, rue Pierre et Marie Curie, 75231 Paris cedex 05, France
[c] Shenyang National Laboratory for Materials Science, Institute of Metal Research, Chinese Academy of Sciences, 72 Wenhua Road, Shenyang 110016, China
[d] INSA de Rennes, UMR CNRS 6226 Sciences Chimiques de Rennes/Chimie- Métallurgie, 20, Avenue des Buttes de Coesmes, 35043 Rennes cedex, France
[e] Laboratoire d'Etude des Textures et Application aux Matériaux LETAM (CNRS- FRE 3143), Université de Metz, France.

ARTICLE INFO

Article history:
Received 16 November 2010
Received in revised form
2 June 2011
Accepted 5 June 2011

Keywords:
Titanium alloys
Thermo-mechanical treatment
Superelasticity
Microstructure
Transmission electron microscopy

ABSTRACT

A flash-thermal treatment technique has been developed very recently to improve both the critical stress to induce the martensitic transformation (MT) and the recoverable deformation of the metastable β type titanium alloys. In this paper, this strategy is applied to both Ti–26Nb and Ti–20Nb–6Zr (at.%) alloys. Since both alloys have identical martensite start (Ms) temperature, it makes possible to investigate the effect of Zr on mechanical properties after the flash-thermal treatment. It is clearly shown that a flash treatment of 360 s at 873 K on heavily cold-rolled samples results in good balance between the tensile strength, the ductility and the recoverable strains. Such contribution is more significant in the ternary alloy in which balanced properties combining high martensitic critical stress over 400 MPa and the large fully recoverable strains up to 3.0% can be achieved. These improvements are due to the flash treatment effects, resulting in ultra-fine β grains with sizes 1–2 μm with nano-sized α and ω phases precipitation in the β matrix.

1. Introduction

Due to low elastic modulus and superelastic deformation behavior, the metastable β type titanium alloys have been widely investigated as a replacement for NiTi shape memory alloys in biomedical applications (Banerjee et al., 2005; Kim et al., 2004a,b, 2006a,b,c; Laheurte et al., 2010; Miyazaki et al., 2006). Most of the work has been focused on Ti–Nb based alloys to characterize the reversible martensitic transformation (MT) between the β parent phase and the α'' martensite and its influence on the mechanical properties, shape memory effect (SME) and superelastic deformation behavior (Banerjee et al., 2004; Niinomi, 2003; Saito et al., 2003; Yamada, 1992). These achievements brought a better understanding of the

* *Corresponding author.* Tel.: +33 1 44 27 67 09.
E-mail address: fredericprima@chimie-paristech.fr (F. Prima).

1751-6161/$ - see front matter © 2011 Published by Elsevier Ltd
doi:10.1016/j.jmbbm.2011.06.003

reversible MT in that category of materials for further development of new improved superelastic alloys. As to the binary Ti–Nb alloys, it is clear that the Ms temperature decrease with the increase of Nb contents following a linear dependence (Kim et al., 2006a,b,c). The Ms temperature is close to the room temperature with the addition of 26 at.% Nb (Kim et al., 2006a,b,c; Miyazaki et al., 2006). As a result, large recoverable strains can be obtained from the stress-induced MT. The superelastic properties can be improved by adding other alloying elements such as Ta, Zr, Sn, Al and/or interstitial elements such as O and N (Abdel-Hady et al., 2007; Fukui et al., 2004; Gloriant et al., 2006, 2008; Hao et al., 2005; Kim et al., 2005, 2006a,b,c; Li et al., 2008; Ping et al., 2005; Sun et al., 2010b; Wang et al., 2008; Xu et al., 2009). An interesting point has been noted concerning both Zr and Sn, these two elements belong to neutral elements due to their weak effect on β transus temperature but depress significantly the Ms temperature as combined with large amount of Nb (Hao et al., 2005; Wang et al., 2008; Xu et al., 2009). Since Zr addition in Ti–Nb alloys has been shown to improve the SME and the superelasticity by the increase of phase transformation strains (Abdel-Hady et al., 2006, 2007; Kim et al., 2005), Ti–Nb–Zr ternary alloys have a promising potential for biomedical applications.

Besides the alloy design, appropriate microstructures are also necessary to optimize the balance between high strength and large recoverable strains. Recently, different kinds of strategies have been used aiming at the refinement of the microstructural scales when compared to the conventional high-temperature annealing treatments. Two steps aging treatments have been successfully experienced in Ti–Nb alloys with good results in terms of strength and superelasticity (Kim et al., 2006a,b,c). Ultra-fined grains have been produced on Ti2448 alloy (Ti–24Nb–4Zr–7.9Sn wt.%) by heavy warm rolling at ~473 K resulting in the combination of high tensile strength and a maximum recoverable strain of about 3% (Li et al., 2008). Very recently, the present authors have presented a strategy based on "flash" recrystallization process produced by a very short thermal treatment on heavily cold-rolled samples (Sun et al., 2010b). This flash treatment strategy has been shown to be very efficient in decreasing the microstructural scale, keeping grain size at about 1 μm with nanoscaled precipitation of both ω and α phases.

In this paper, we focused on the Zr influence on superelastic properties regarding the flash treatment strategy. The effect of this approach on a binary Ti–26Nb (at.%) alloy and a ternary Ti–20Nb–6Zr alloy have been compared with respect to their microstructure and mechanical properties. Zr and Nb elements have previously shown to display similar effect on decreasing Ms temperature (Kim et al., 2005, 2006a,b,c; Xu et al., 2009). However, they play a different role in the high temperature stability of the beta phase (i.e, T_β, the β-transus temperature). Zr is known as a neutral element with no influence on T_β whereas Nb behaves as a classical β stabilizer decreasing T_β temperature. As a consequence, equiatomic substitution of Nb element by Zr element results in an increase of T_β temperature of about 70 K keeping the Ms temperature at the same level. Therefore, in that work, two samples with comparable Ms temperature but different β stability are compared regarding their microstructural and mechanical responses when subjected to identical thermo-mechanical treatments (heavy cold rolling and flash treatment).

2. Experimental setup

The ingots of Ti–26Nb (at.%) and Ti–20Nb–6Zr (at.%) about 25 g were first melted by cold crucible levitation melting (CCLM) furnace using pure metals, then remelted three times in an arc melting furnace and finally formed into cylinders. Homogenization treatment at 1173 K was held under high vacuum of 10^{-6} Pa for 20 h followed by water quenching. The as-quenched ingots were heavily cold-rolled 90% to 0.5 mm in thickness. Additional solution treatment was performed on some cold-rolled materials at 1143 K for 30 min to obtain fully recrystallized large grained structure for XRD references. In order to characterize the phase transformation temperatures of Ti–20Nb–6Zr, the differential scanning calorimetric (DSC) measurement was applied by using METTLER TOLEDO DSC 822e equipment at the rate of 20 K/min to determine the M_s and A_f temperatures. For the transformations happened at the temperature range 300–1200 K, the relative electrical resistivity measurement (ERM) was performed by using four-probe method under vacuum at a heating rate of 5 K/min. Tensile specimens were mechanically prepared from the as-rolled sheet with gage dimension $30 \times 4 \times 0.5$ mm^3 along the rolling direction (RD). They were sealed in a silica tube with pure helium gas to avoid contamination, immersed into a pre-heated salt bath of 873 K for a short time of 360 s and finally quenched into water. After the above flash-thermal treatment (Sun et al., 2010b), the uniaxial cyclic tensile tests with a total strain of 3.5% at an interval of 0.5% were performed at room temperature with an initial strain rate of 1.1×10^{-3} s^{-1}. Single step tensile tests were also performed to measure ductility of the as-rolled and flash-treated specimens. To ensure accuracy of the above measurements, the stress–strain curves were recorded by a calibrated extensometer. X-ray diffraction (XRD) was performed by using Phillips PW3710 with Cu$K\alpha$ radiation operating at 30 kV and 20 mA. Transmission electron microscopy (TEM) of JEOL 2000FX operating at 200 kV was used for microstructure observations.

3. Results

3.1. *Phase constitution and microstructure*

After the heavy cold rolling with a thickness reduction of 90%, the XRD analyses are conducted to characterize the phase constitutions of both alloys (Fig. 1(a)). From that figure, it can be evidenced that the cold rolling process results in a large amount of the α'' martensite in both Ti–26Nb binary alloy (Fig. 1(a)) and Ti–20Nb–6Zr ternary alloy (Fig. 1(a)). After solution treatment at 1143 K followed by quenching, a single β phase can be identified (Fig. 1(b)), indicating that martensite is stress/strain-induced during cold rolling. The XRD profiles also showed significant peak broadening (comparing to ST samples in Fig. 1(b)) corresponding to a large accumulation of microstrains and evolution of the defect structures leading to a drastic decrease of the coherent domain sizes. Some differences can be noted both from XRD and from TEM investigation. From XRD traces, it can be seen that there is a difference regarding the crystallographic texture. The cold-rolled Ti–26Nb sample displays a $(200)_\beta$ texture whereas, in

Please cite this article in press as: Sun, F., et al., A thermo-mechanical treatment to improve the superelastic performances of biomedical Ti–26Nb and Ti–20Nb–6Zr (at.%) alloys. Journal of the Mechanical Behavior of Biomedical Materials (2011), doi:10.1016/j.jmbbm.2011.06.003

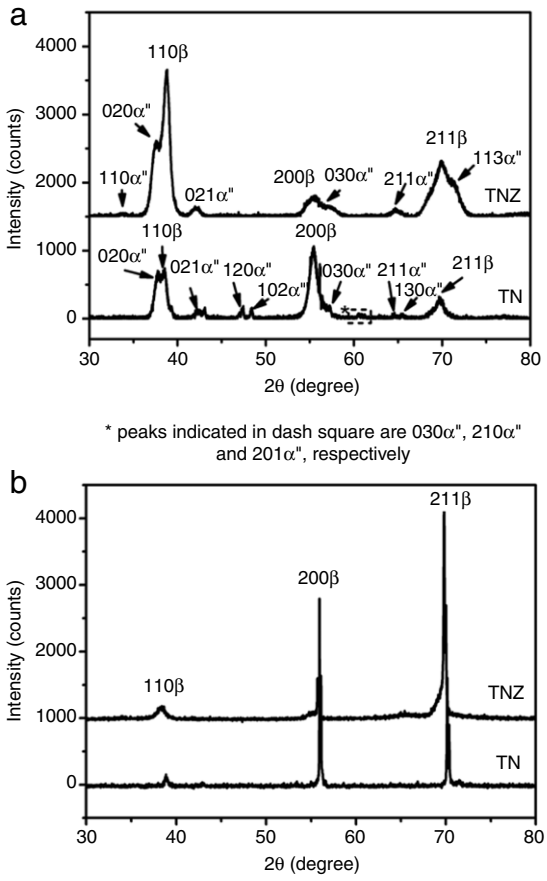

Fig. 1 – XRD results of Ti–20Nb–6Zr (TNZ) and Ti–26Nb (TN) subjected to heavy cold rolling (a) and subjected to solution treatment as references (b).

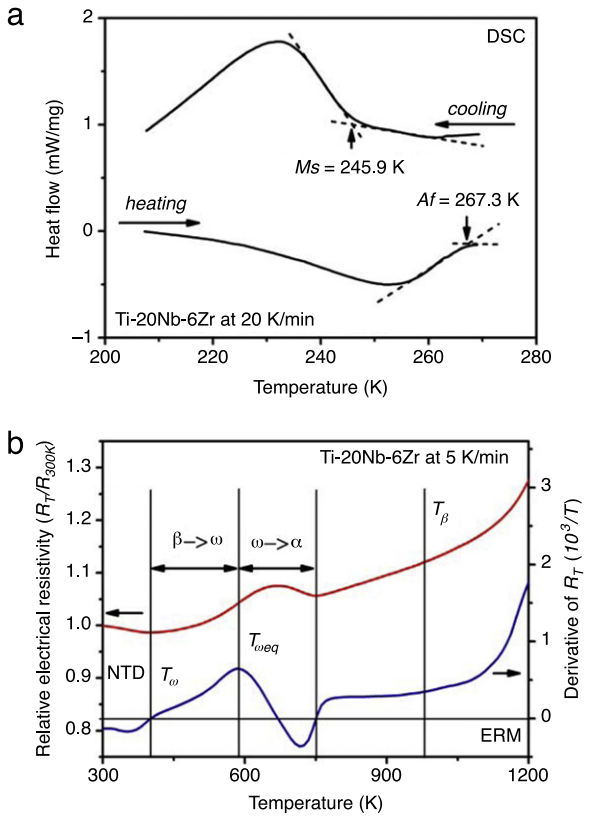

Fig. 3 – Phase transformation analysis of Ti–20Nb–6Zr in the range of 200–1200 K: DSC measurements at a rate of 20 K/min (a) and relative electrical resistivity measurement (ERM) at 5 K/min.

Ti–20Nb–6Zr alloy, the deformation texture remains rather weak. TEM observations show that the cold deformation process gives birth to a large density of dislocations in both cases but differences are notable concerning the defects structure. Ti–26Nb deformed structure reveals elongated cell blocks separated by lamellar dislocation boundary structures whereas in Ti–20Nb–6Zr, misorientation is spread among ultra-fine equiaxed subgrain structures. The α'' martensite is also detected by TEM analyses in cold-rolled Ti–26Nb alloys from the diffraction pattern (inset in Fig. 2(a)) along $[113]_\beta$ zone axis with diffused α'' spots. However, in Ti–20Nb–6Zr alloy, the continuous diffraction rings (inset of Fig. 2(b)) are observed due to the uniform fine structure (Fig. 2(b)), where the labeled α'' spot is not very clear because of its superposition onto the $(110)_\beta$ diffraction ring. Generally, the existence of α'' phase are explicit from XRD profiles in both alloys but less significant in small scale TEM analysis due to the complex deformation microstructure. TEM analysis also found the ω phase in the binary Ti–26Nb alloy, as evidenced by the inserted SAD pattern in Fig. 2(a). ω phase in the ternary Ti–20Nb–6Zr alloy is difficult to be identified due to the continual diffraction rings (Fig. 2(b)).

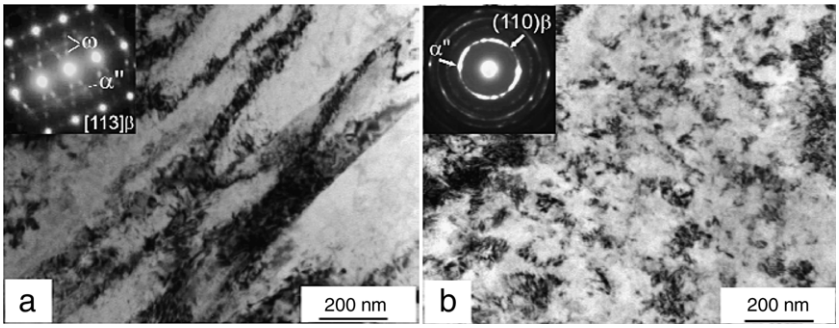

Fig. 2 – Bright field TEM images of as-rolled Ti–26Nb (a) and Ti–20Nb–6Zr (b) with corresponding diffraction patterns.

Please cite this article in press as: Sun, F., et al., A thermo-mechanical treatment to improve the superelastic performances of biomedical Ti–26Nb and Ti–20Nb–6Zr (at.%) alloys. Journal of the Mechanical Behavior of Biomedical Materials (2011), doi:10.1016/j.jmbbm.2011.06.003

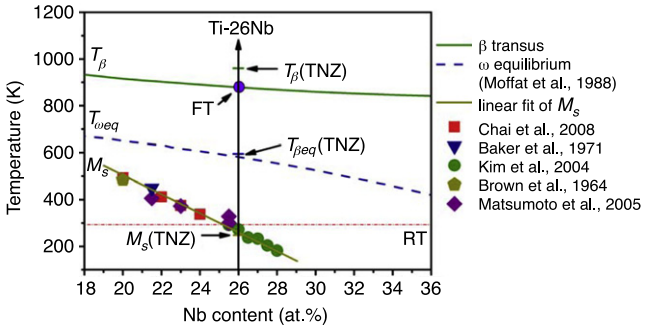

Fig. 4 – Dependence of phase transformation temperatures on Nb content in Ti–Nb alloy with comparison between Ti–26Nb and Ti–20Nb–6Zr alloys. (Baker, 1971; Brown et al., 1964; Chai et al., 2008; Matsumoto et al., 2005; Moffat and Kattner, 1988).

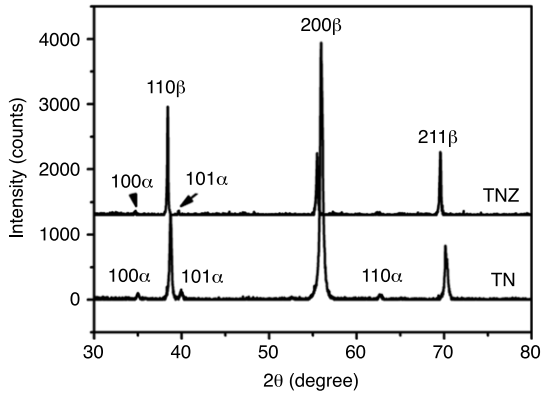

Fig. 5 – XRD results of Ti–20Nb–6Zr (TNZ) and Ti–26Nb (TN) subjected to flash-treatment at 873 K for 360 s.

In order to characterize the phase transformation sequence of the Ti–20Nb–6Zr alloy, DSC and ERM methods were performed to analyze the critical phase transformation temperatures (Fig. 3). From the results of DSC measurement, the martensitic transformation (MT) temperature was determined to be about 246 K (Fig. 3(a)). The phase transformation temperatures at the range between 300 and 1200 K were analyzed by ERM methods at a heating rate of 5 K/min (Fig. 3(b)). A typical β metastable Ti-alloy curve was obtained by starting with negative temperature dependence (NTD) effect, which was probably related to the ω_{ath} phase transformation (Gloriant et al., 2008). The critical transformation temperatures of β/ω, ω/α and β transus were determined and plotted versus those of Ti–26Nb alloy on Fig. 4. It can be clearly noted that the Ms of both alloys is almost equal, which is in good accordance with the equiatomic substitution strategy utilized in this study.

After the flash-thermal treatment at 873 K in the $(\alpha + \beta)$ phase field for 360 s, the XRD profiles in Fig. 5 showed that both alloys contained the major β phase and a little amount of α phase. It can be noted that the stress-induced α'' phase is entirely reversed during the short time thermal treatment. TEM observations show that the β grains exhibit an ultra-fine microstructure in both Ti–26Nb (Fig. 6) and Ti–20Nb–6Zr alloys (Fig. 7). It should be noted that most β grains remain rather elongated with low angle boundaries in the Ti–26Nb alloy, probably resulting from an uncompleted recrystallization. For the Ti–20Nb–6Zr alloy, the β grains appear uniformly sized in equiaxed shape and an average size of 1–2 μm. These microstructural features show the promising potential of extremely short thermal treatments for titanium alloys. In the case of superelastic alloys, it is reasonable to assume that the reversion of the stress-induced α'' into β phase during the short time treatment plays a key role in the recrystallization kinetics. This means that an appropriate flash-thermal treatment can allow suppression of excessive β grains growth. Furthermore, TEM investigation (Figs. 6 and 7) reveals that the two systems display nanoscaled microstructure after the flash treatment. A fine plate-shaped α phase of hundreds of nanometers in length is observed while a nano-sized ω phase is distributed uniformly in the β matrix. It can be noted from the TEM images that the volume fraction of both ω and α phases may be higher in the Ti–20Nb–6Zr than in the Ti–26Nb. The thermokinetics of the nucleation and growth of ω phase has been discussed in our previous research (Sun et al., 2010a). Additionally, a nano-sized α phase formed, probably in relation with ω sites is also observed in both alloys, which is in accordance with the previous research (Azimzadeh and Rack, 1998; Prima et al., 2000, 2006). Therefore, the flash treatment strategy results in a drastic reduction of the whole microstructure (grain size and phase precipitation) in these titanium alloys.

3.2. *Tensile tests*

The stress–strain curves upon single loading tests before and after the flash-thermal treatment are reported in Fig. 8. Both cold-rolled materials exhibit low ductility with higher tensile stress for the Ti–20Nb–6Zr alloy compared to the Ti–26Nb alloy. The flash treatment results in significant improvement of ductility and a decrease of tensile strength, with appearance of a typical "double yielding" phenomenon with a flat plateau corresponding to the precipitation of a stress-induced martensitic transformation. When compared with the previous results on Ti–Nb–(Zr, Ta, Mo) alloys (Table 1), the flash treatment is shown to be promising with good combination of high tensile strength (~680 MPa for the Ti–Nb–Zr) and superelasticity. As a matter of comparison, the maximum reported values for UTS after conventional solution treatment at 1173 K are 450 MPa in superelastic Ti–Nb–Zr alloys.

The single loading tests are completed by cyclic loading tests on both flash-treated materials. The elastic deformation behavior and the recoverable tensile strains are evaluated (Fig. 9). The flash treatment has the advantage of improving the recoverable strain to ~2.3% and ~3.2% for the binary and ternary alloy, respectively (Fig. 10). The variations of recoverable strains with the applied tensile strains are plotted in Fig. 11. It is clear that the flash-treated ternary alloy has the largest fully recoverable strains up to 3%. Together with its high value of critical stress ~410 MPa (Fig. 10), this material displays a great potential for biomedical applications. For example in the dental applications, the material for orthodontic wires requires appropriate superelasticity to adapt the applied strain and provide efficient correction stress upon

Please cite this article in press as: Sun, F., et al., A thermo-mechanical treatment to improve the superelastic performances of biomedical Ti–26Nb and Ti–20Nb–6Zr (at.%) alloys. Journal of the Mechanical Behavior of Biomedical Materials (2011), doi:10.1016/j.jmbbm.2011.06.003

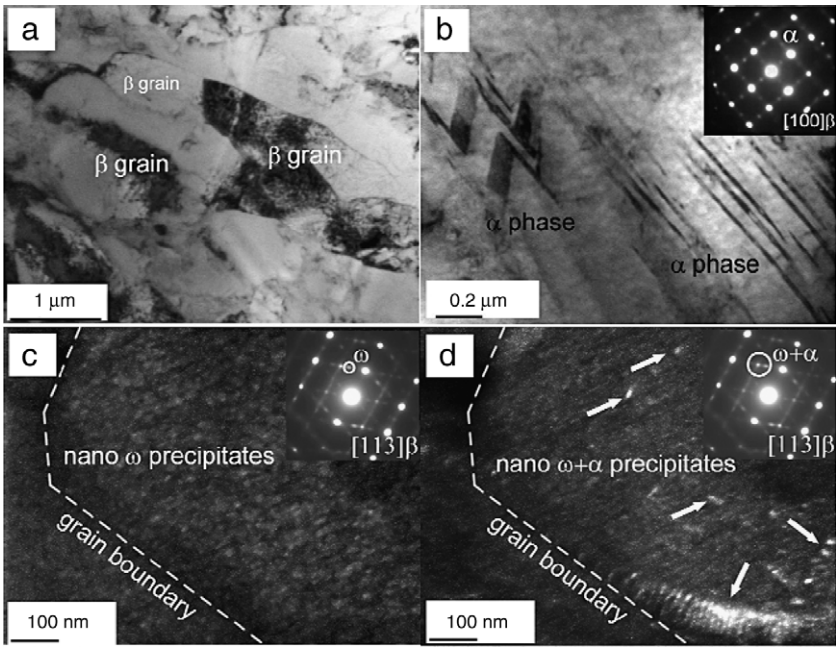

Fig. 6 – TEM images of flash-treated Ti–26Nb of bright field image of β grains (a), bright field image of large α bands (b), dark field image of ω precipitates in a single grain (c) and dark field image of $\omega + \alpha$ precipitates in a single grain (d) with corresponding diffraction patterns.

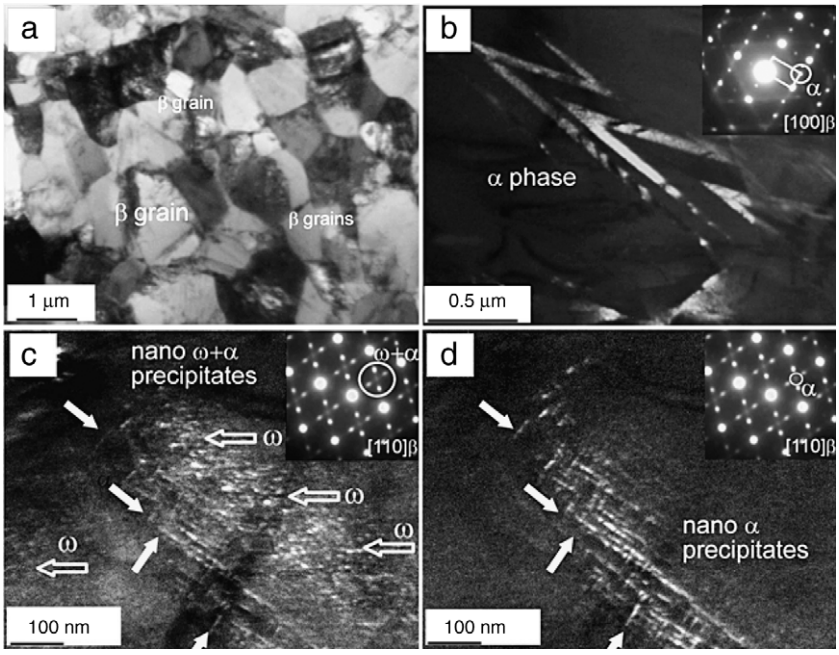

Fig. 7 – TEM images of flash-treated Ti–20Nb–6Zr of bright field image of β grains (a), bright field image of large α bands (b), dark field image of ω (open arrows) $+\alpha$ (solid arrows) precipitates in a single grain (c) and dark field image of α precipitates (solid arrows) in the same area (d) with corresponding diffraction patterns.

strain recovery process. Generally, Ni–Ti based superelastic alloys fulfill the mechanical requirements but suffer important cyto-toxic risks due to the hyper-sensitized Ni element in certain group of people. Ti–Nb or Ti–Nb–Zr alloy systems consist of non-toxic elements Ti, Nb and Zr and the cyto-toxicity of the alloys is equivalent to that of pure Ti (Majumdar et al., 2011; Miyazaki et al., 2006; Niinomi, 2003). The martensitic phase transformation plateau is indicated in the figure by black arrows. The martensitic range of Ti–20Nb–6Zr is 2.5% compared to 1.7% of Ti–26Nb. The martensitic deformation ranges of both alloys are different due to the strain misfit between β/α'' phase (Miyazaki et al., 2006).

Please cite this article in press as: Sun, F., et al., A thermo-mechanical treatment to improve the superelastic performances of biomedical Ti–26Nb and Ti–20Nb–6Zr (at.%) alloys. Journal of the Mechanical Behavior of Biomedical Materials (2011), doi:10.1016/j.jmbbm.2011.06.003

Table 1 – Mechanical performances at room temperature of recently developed superelastic Ti–Nb based alloys subjected to single thermal treatment.

Alloys	Thermal treatments	CRSS SIM (MPa)	Maximum recovery rate @ applied strain (%) and stress (MPa)	Recovery rate from 3% prestrain @ applied stress (MPa)	Complete recovery range (%)	References
Ti–26Nb[a]	ST/1173 K/1800 s	140	49%@4.0(430)	60%@207	<1.5	Kim et al., 2004a,b
Ti–26Nb[a]	AG/873 K/600 s	134	58%@4.0(534)	73%@211	<1.5	Kim et al., 2006a,b,c
Ti–26Nb	FT/873 K/360 s	270	77%@3.0(628)	77%@628	<2.0	Present work
Ti–27Nb[a]	AG/973 K/1800 s	190	69%@3.5(437)	77%@387	<1.5	Kim et al., 2006a,b,c
Ti–20Nb–6Zr	ST/1143 K/1800 s	248	71%@3.5(527)	80%@486	<2.0	Present work
Ti–20Nb–6Zr	FT/873 K/360 s	410	91%@3.5(682)	100%@578	<3.5	Present work
Ti–22Nb–6Zr[a]	ST/1173 K/1800 s	171	88%@4.0(285)	95%@222	<1.5	Kim et al., 2005
Ti–22Nb–6Ta[a]	ST/1173 K/1800 s	167	58%@3.6(436)	60%@400	<1.5	Miyazaki et al., 2006
Ti–18Nb–3Mo[a]	AG/973 K/1800 s	341	85%@4.0(462)	96%@401	<1.5	Al-Zain et al., 2010

[a]Supplementary heating at ~500 K were preformed after certain cyclic unloading processes.

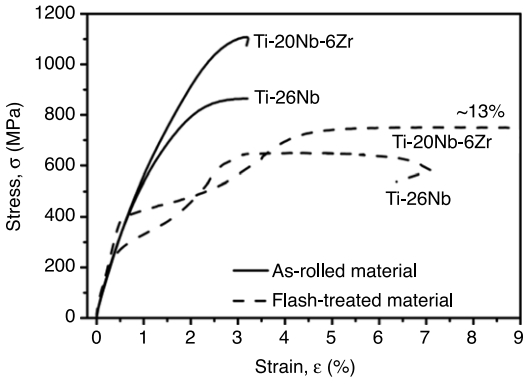

Fig. 8 – Tensile results of single loading tests on Ti–26Nb and Ti–20Nb–6Zr before (solid lines) and after (dash lines) flash-thermal treatments, respectively.

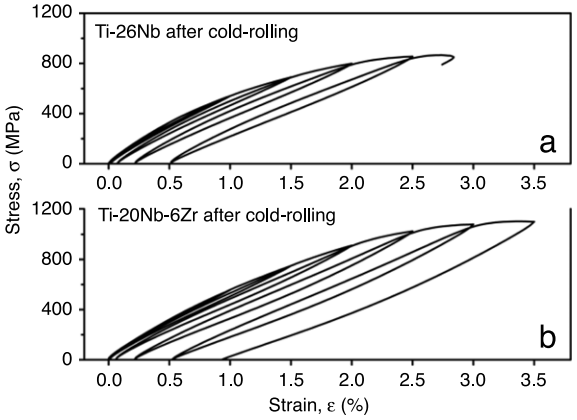

Fig. 9 – Incremental loading–unloading tensile curves of as-rolled Ti–26Nb (a) and Ti–20Nb–6Zr (b) at room temperature.

3.3. *Microstructure after the cyclic deformation*

After the cyclic tests using tensile strains up to 3.5%, TEM specimens are prepared for microstructural observations and the results are reported in Figs. 12 and 13. The stress-induced α'' martensite can be easily found using SAD patterns in both alloys, while the dark field observations showed the α'' plate-shaped martensite inside β grains. Interestingly, a number of regular SIM α'' layers with thickness ~200 nm arranged parallel in a β grain with size ~2 μm are found in the Ti–20Nb–6Zr ternary alloy (Fig. 13(a)). In detail, the internal twinning involved in the martensitic transformation is also detected in the corresponding SAD pattern (Fig. 13(b)) along $[11\text{-}2]_{\alpha''}$ zone axis, which is consistent with the previous reports (Nag et al., 2009).

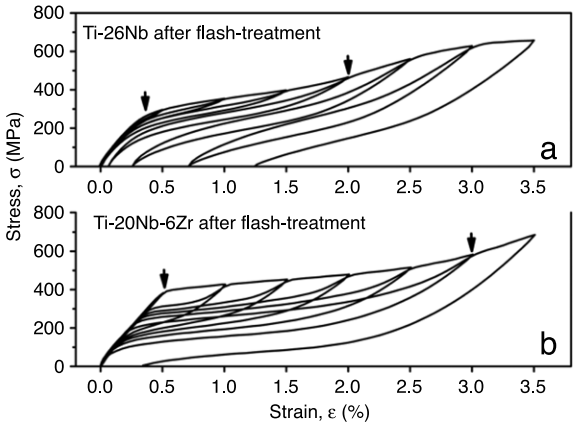

Fig. 10 – Incremental loading–unloading tensile curves of flash-treated Ti–26Nb (a) and Ti–20Nb–6Zr (b) at room temperature, the yielding ranges of stress-induced martensite are indicated by black arrows.

4. Discussion

Equiatomic substitution of 6 at.% Nb by Zr element induces notable changes both in the defects structure of cold-rolled materials and recrystallization kinetics since flash-treated microstructure is made of well recrystallized β grains with high angle dislocation boundaries in the case of Ti–20Nb–6Zr (Fig. 7) whereas incomplete recrystallization is visible on Ti–26Nb from Fig. 6. The initial structure from as-rolled states essentially influences the "reconstruction" process of β matrix when subjected to flash-thermal treatment. These differences regarding the dislocation boundaries are interesting

Please cite this article in press as: Sun, F., et al., A thermo-mechanical treatment to improve the superelastic performances of biomedical Ti–26Nb and Ti–20Nb–6Zr (at.%) alloys. Journal of the Mechanical Behavior of Biomedical Materials (2011), doi:10.1016/j.jmbbm.2011.06.003

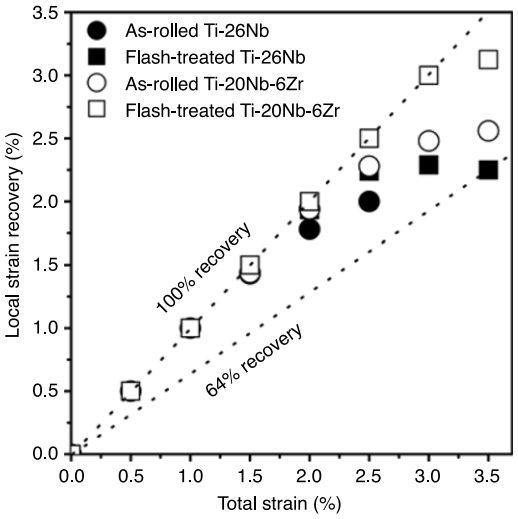

Fig. 11 – The diagram of local strain recovery versus total strain of all specimens.

since little information is available in the literature about these mechanisms in BCC metals. Preliminary assumption that the equiatomic substitution of Nb by Zr could have a beneficial advantage in modifying the stacking fault energy (SFE) of the material resulting in changes of the dislocation boundaries after the cold rolling process and leading to a very refined structure similar to those observed in severe plastic deformation approaches such as Equal Channel Angular Processing (ECAP) (Xu et al., 2009) can be made. However, local crystallographic information would be actually needed to emphasize this assumption. In detail, two hypotheses can be made to explain these differences. (1) The equiatomic substitution of Nb by Zr may result in a variation of the SFE of the material which induces a subsequent adaptation of the defect structure and dislocation boundaries. This could explain an increased nucleation rate of new β grains in Ti–Nb–Zr alloy during the flash treatment. (2) It can be hypothesized that the volume fraction of stress-induced martensite α'' is increased during the cold rolling sequence when Nb is substituted by Zr. It is presently thought that the recrystallization is actually "assisted" by the phase reversion from α'' to β during the thermal treatment, meaning the recrystallization kinetics (the nucleation of new beta grains) could be partially dependent on the initial volume fraction of α'' phase. These two complementary hypotheses could explain the differences regarding the compared grain size and structures in the two systems, after the thermal treatment. On the experimental XRD traces (Fig. 5), it can be noted that a higher volume fraction of α phase is induced by the flash treatment in the Ti–26Nb alloy. Different effects have to be taken into account. In one hand, considering the respective β stabilizing effect of Nb and Zr, the α phase volume fraction in Ti–Nb–Zr should be higher than in the Ti–Nb material. Actually, even if they play the same role in decreasing the Ms temperature in titanium alloys, Zr element is traditionally considered as a neutral element regarding the precipitation of α phase. However, on the

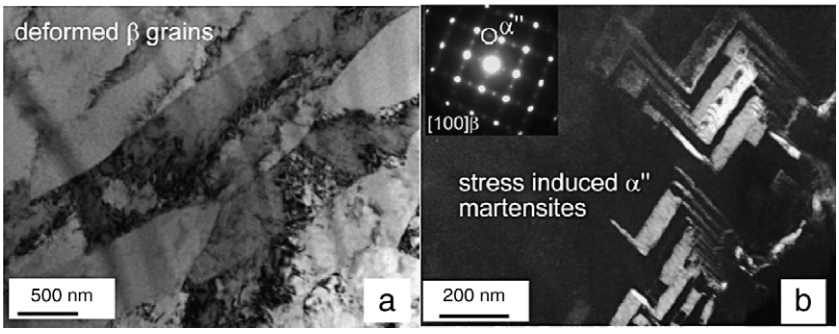

Fig. 12 – TEM images of flash-treated Ti–26Nb after 3.5% deformation, (a) bright field images of β matrix, (b) dark field image of stress-induced α'' martensites and corresponding diffraction pattern.

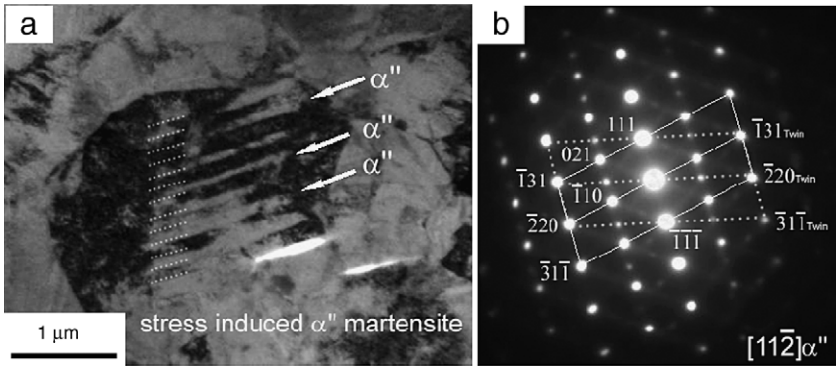

Fig. 13 – TEM images of flash-treated Ti–20Nb–6Zr after 3.5% deformation, (a) bright field images of a single β grain, (b) the corresponding diffraction pattern.

Please cite this article in press as: Sun, F., et al., A thermo-mechanical treatment to improve the superelastic performances of biomedical Ti–26Nb and Ti–20Nb–6Zr (at.%) alloys. Journal of the Mechanical Behavior of Biomedical Materials (2011), doi:10.1016/j.jmbbm.2011.06.003

other hand, the respective position of the aging temperature in Fig. 4 is quite different from one to another alloy since they display different T_β temperatures (T_β = 880 K for Ti–Nb alloy and T_β = 950 K for Ti–Nb–Zr alloy). Therefore, the same aging temperature can result in notable differences concerning the α volume fraction. During the flash-thermal treatment, alloying elements are locally redistributed between the two phases α and β. This increased precipitation may result in a local chemical enrichment of the β matrix in β stabilizer elements (Niobium) and a subsequent decrease of Ms temperature. Moreover, we suggest that an increased volume fraction of α phase will result in a progressive disappearance of the superelastic effect by a combined effect of chemical stabilization of beta phase and a detrimental elastic interaction with stress-induced α'' platelets (on precipitation and reversion). In comparison, Ti–20Nb–6Zr demonstrates excellent structural responses on cold-working and flash treatment. The positive effects of adding Zr is consistent and have been already reported in the previous studies (Abdel-Hady et al., 2006, 2007; Kim et al., 2005); however the mechanism of action of this element was unclear. In this investigation, addition of Zr element leads to a decrease of the high temperature β phase stability, increasing the β transus by 70 K (from 880 K for Ti–26Nb) but keep the Ms temperature when compared to Ti–26Nb (~250 K). It displays an excellent combination of strength and superelasticity due to an extremely efficient recrystallization and a very fine precipitation scale at the nanoscale level. As reported before (Ankem and Greene, 1999; Sun et al., 2010c), the nanostructuration involving ω and/or α precipitation is efficient in structural strengthening of metastable β alloys and constitutes one of the most interesting microstructural features of the flash-thermal treatment.

For every system subjected to flash-thermal treatment, an ideal compromise has to be found (in terms of time and temperature) between the recrystallization kinetics and the phase precipitation kinetics. From this investigation, submicrometric β grains combined with tiny particles of ω and α phases (promoting the nucleation, but drastically limiting the growth of these particles) seem to be optimal to reach excellent balance of strength and superelastic properties.

5. Conclusion

Ti–26Nb and Ti–20Nb–6Zr alloys having identical Ms temperatures are subjected to heavy cold rolling with thickness reduction of 90% and then the flash-thermal treatment at 873 K for 360 s. The microstructural observations and the cyclic tensile tests at room temperature draw the following conclusions.

(1) The heavy cold rolling produces more uniform nanostructured subgrains in the ternary alloy than in the binary alloy. The cold-rolled alloys with ($\beta + \alpha''$) microstructures exhibit nonlinear elastic deformation behavior but bad ductility.

(2) The flash-thermal treatment results in the ultra-fine β grains with sizes 1–2 μm as well as the nano-sized α and ω phases in the β matrix. A complete recrystallization is observed in the Ti–Nb–Zr alloy but not in the Ti–Nb alloy.

(3) The flash-thermal treatment adopted in this study is more effective to improve the critical stress to induce the MT and the recoverable strains by the replacement of Zr to Nb. Both high critical stress ~410 MPa and the large fully recoverable strains ~3.0% can be reached. The treatment also enhances the ductility of both alloys significantly.

Acknowledgment

This work was supported by the French National Research Agency (No. ANR 08MAPR 0017).

REFERENCES

Abdel-Hady, M., Fuwa, H., Hinoshita, K., Kimura, H., Shinzato, Y., Morinaga, M., 2007. Phase stability change with Zr content in β-type Ti–Nb alloys. Scr. Mater. 57, 1000–1003.

Abdel-Hady, M., Henoshita, K., Morinaga, M., 2006. General approach to phase stability and elastic properties of β-type Ti-alloys using electronic parameters. Scr. Mater. 55, 477–480.

Al-Zain, Y., Kim, H.Y., Hosoda, H., Nam, T.H., Miyazaki, S., 2010. Shape memory properties of Ti–Nb–Mo biomedical alloys. Acta Mater. 58, 4212–4223.

Ankem, S., Greene, C.A., 1999. Recent developments in microstructure/property relationships of beta titanium alloys. Mater. Sci. Eng. A 263, 127–131.

Azimzadeh, S., Rack, H.J., 1998. Phase transformations in Ti–6.8Mo–4.5Fe–1.5Al. Metall. Mater. Trans. A 29, 2455.

Baker, C., 1971. The shape-memory effect in a titanium–35 wt% niobium alloy. Met. Sci. J. 5, 92–100.

Banerjee, R., Nag, S., Fraser, H.L., 2005. A novel combinatorial approach to the development of beta titanium alloys for orthopaedic implants. Mater. Sci. Eng. C 25, 282–289.

Banerjee, R., Nag, S., Stechschulte, J., Fraser, H.L., 2004. Strengthening mechanisms in Ti–Nb–Zr–Ta and Ti–Mo–Zr–Fe orthopaedic alloys. Biomaterials 25, 3413–3419.

Brown, A.R.G., Clark, D., Eastabrook, J., Jepson, K.S., 1964. The titanium–niobium system. Nature 201, 914–915.

Chai, Y.W., Kim, H.Y., Hosoda, H., Miyazaki, S., 2008. Interfacial defects in Ti–Nb shape memory alloys. Acta Mater. 56, 3088–3097.

Fukui, Y., Inamura, T., Hosoda, H., Wakashima, K., Miyazaki, S., 2004. Mechanical properties of a Ti–Nb–Al shape memory alloy. Mater. Trans. 45, 1077–1082.

Gloriant, T., Texier, G., Prima, F., laillé, D., Gordin, D.M., Thibon, I., Ansel, D., 2006. Synthesis and phase transformations of beta metastable Ti-based alloys containing biocompatible Ta, Mo and Fe beta-stabilizer elements. Adv. Eng. Mater. 8, 961.

Gloriant, T., Texier, G., Sun, F., Thibon, I., Prima, F., Soubeyroux, J.L., 2008. Characterization of nanophase precipitation in a metastable β titanium-based alloy by electrical resistivity, dilatometry and neutron diffraction. Scr. Mater. 58, 271.

Hao, Y.L., Li, S.J., Sun, S.Y., Zheng, C.Y., Hu, Q.M., Yang, R., 2005. Super-elastic titanium alloy with unstable plastic deformation. Appl. Phys. Lett. 87, 091906.

Kim, H.Y., Hashimoto, S., Kim, J.I., Inamura, T., Hosoda, H., Miyazaki, S., 2006a. Effect of Ta addition on shape memory behavior of Ti–22Nb alloy. Mater. Sci. Eng. A 417, 120–128.

Kim, H.Y., Kim, J.I., Inamura, T., Hosoda, H., Miyazaki, S., 2006b. Effect of thermo-mechanical treatment on mechanical properties and shape memory behavior of Ti–(26–28) at.% Nb alloys. Mater. Sci. Eng. A 438–440, 839–843.

Kim, H.Y., Sasaki, T., Okutsu, K., Kim, J.I., Inamura, T., Hosoda, H., Miyazaki, S., 2006c. Martensitic transformation, shape memory effect and superelasticity of Ti–Nb binary alloys. Acta Mater. 54, 2419–2429.

Please cite this article in press as: Sun, F., et al., A thermo-mechanical treatment to improve the superelastic performances of biomedical Ti–26Nb and Ti–20Nb–6Zr (at.%) alloys. Journal of the Mechanical Behavior of Biomedical Materials (2011), doi:10.1016/j.jmbbm.2011.06.003

Kim, H.Y., Ohmatsu, Y., Kim, J.I., Hosoda, H., Miyazaki, S., 2004a. Mechanical properties and shape memory behavior of Ti–Mo–Ga alloys. Mater. Trans. 45, 1090–1095.

Kim, H.Y., Satoru, H., Kim, J.I., Hosoda, H., Miyazaki, S., 2004b. Mechanical properties and shape memory behavior of Ti–Nb alloys. Mater. Trans. 45, 2443–2448.

Kim, J.I., Kim, H.Y., Inamura, T., Hosoda, H., Miyazaki, S., 2005. Shape memory characteristics of Ti–22Nb–(2–8)Zr (at.%) biomedical alloys. Mater. Sci. Eng. A 403, 334–339.

Laheurte, P., Prima, F., Eberhardt, A., Gloriant, T., Wary, M., Patoor, E., 2010. Mechanical properties of low modulus β titanium alloys designed from the electronic approach. J. Mech. Behav. Biomed. Mater. doi:10.1016/j.jmbbm.2010.07.001.

Li, S.J., Cui, T.C., Li, Y.L., Hao, Y.L., Yang, R., 2008. Ultrafine-grained β-type titanium alloy with nonlinear elasticity and high ductility. Appl. Phys. Lett. 92, 043128.

Majumdar, P., Singh, S.B., Chakraborty, M., 2011. The role of heat treatment on microstructure and mechanical properties of Ti–13Zr–13Nb alloy for biomedical load bearing applications. J. Mech. Behav. Biomed. Mater. doi:10.1016/j.jmbbm.2011.03.023.

Matsumoto, H., Watanabe, S., Hanada, S., 2005. Beta TiNbSn alloys with low Young's modulus and high strength. Mater. Trans. 46, 1070–1078.

Miyazaki, S., Kim, H.Y., Hosoda, H., 2006. Development and characterization of Ni-free Ti-base shape memory and superelastic alloys. Mater. Sci. Eng. A 438–440, 18–24.

Moffat, D.L., Kattner, U.R., 1988. The stable and metastable Ti–Nb phase diagrams. Metal. Trans. A 9, 1988–2389.

Nag, S., Banerjee, R., Srinivasan, R., Hwang, J.Y., Harper, M., Fraser, H.L., 2009. ω-assisted nucleation and growth of α precipitates in the Ti–5Al–5Mo–5V–3Cr–0.5Fe β titanium alloy. Acta Mater. 57, 2136.

Niinomi, M., 2003. Fatigue performance and cyto-toxicity of low rigidity titanium alloy, Ti–29Nb–13Ta–4.6Zr. Biomaterials 24, 2673–2683.

Ping, D.H., Mitarai, Y., Yin, F.X., 2005. Microstructure and shape memory behavior of a Ti–30Nb–3Pd alloy. Scr. Mater. 52, 1287–1291.

Prima, F., Debuigne, J., Boliveau, M., Ansel, D., 2000. Control of omega phase volume fraction precipitated in a beta titanium alloy: Development of an experimental method. J. Mater. Sci. Lett. 19, 2219–2221.

Prima, F., Vermaut, P., Texier, G., Ansel, D., Gloriant, T., 2006. Evidence of α-nanophase heterogeneous nucleation from ω particles in a β-metastable Ti-based alloy by high-resolution electron microscopy. Scr. Mater. 54, 645.

Saito, T., Furuta, T., Hwang, J.H., Kuramoto, S., Nishino, K., Suzuki, N., Chen, R., Yamada, A., Ito, K., Seno, Y., Nonaka, T., Ikehata, H., Nagasako, N., Iwamoto, C., Ikuhara, Y., Sakuma, T., 2003. Multifunctional alloys obtained via a dislocation-free plastic deformation mechanism. Science 300, 464–467.

Sun, F., Laillé, D., Gloriant, T., 2010a. Thermal analysis of the ω nanophase transformation from the metastable β Ti–12Mo alloy. J. Therm. Anal. Calorim. 101, 81–88.

Sun, F., Nowak, S., Gloriant, T., Laheurte, P., Eberhardt, A., Prima, F., 2010b. Influence of a short thermal treatment on the superelastic properties of a titanium-based alloy. Scr. Mater. 63, 1053–1056.

Sun, F., Prima, F., Gloriant, T., 2010c. High-strength nanostructured Ti–12Mo alloy from ductile metastable beta state. Mater. Sci. Eng. A 527, 4262–4269.

Wang, B.L., Zheng, Y.F., Zhao, L.C., 2008. Effects of Sn content on the microstructure, phase constitution and shape memory effect of Ti–Nb–Sn alloys. Mater. Sci. Eng. A 486, 146–151.

Xu, W., Wu, X., Calin, M., Stoica, M., Eckert, J., Xia, K., 2009. Formation of an ultrafine-grained structure during equal-channel angular pressing of a β-titanium alloy with low phase stability. Scr. Mater. 60, 1012–1015.

Yamada, Y., 1992. Theory of pseudoelasticity and the shape-memory effect. Phys. Rev. B 46, 5906–5911.

Please cite this article in press as: Sun, F., et al., A thermo-mechanical treatment to improve the superelastic performances of biomedical Ti–26Nb and Ti–20Nb–6Zr (at.%) alloys. Journal of the Mechanical Behavior of Biomedical Materials (2011), doi:10.1016/j.jmbbm.2011.06.003